Pergamon

Int. J. Mach. Tools Manufact. Vol. 36, No. 10, pp. 1123–1135, 1996

0890-6955/96$15.00 + .00

PII: S0890-6955(96)00020-X

EFFECTS OF THE HOB CUTTER REGRINDING AND SETTING ON ZE-TYPE WORM GEAR MANUFACTURE

HONG-SHENG FANG† and CHUNG-BIAU TSAY†*

(*Original received* 30 *October* 1995)

Abstract—A mathematical model for a ZE-type worm gear set is proposed. The characteristics of a ZE-type worm gear cut with an oversize hob cutter are investigated. Bearing contacts and kinematic errors in the ZE-type worm gear set due to regrinding of oversize hob cutters are also studied. Bearing contacts in the worm gear set were obtained using surface separation topology techniques and tooth contact analysis. It was found that bearing contact locations are sensitive to the hob cutter setting angle and setting distance. Kinematic error minimization was achieved modifying worm normal tooth angle. By applying the optimization theorem and computer simulation programs, optimum hob cutter settings and worm normal tooth angle were determined to improve bearing contact location and minimize the worm gear set kinematic errors. A numerical example is given to demonstrate the results of the investigation. The developed computer-aided manufacture program has successfully been applied to the worm gear manufacture and hob cutter design. Copyright © 1996. Published by Elsevier Science Ltd

1. INTRODUCTION

A worm gear set is composed of a worm and worm gear, and is an important device for transmitting torque between crossed axes. Due to their high transmission ratios, low noise and compact structures, worm gear sets are widely used in gear-reduction mechanisms. According to well-known cutting methods and DIN standards, worm gear sets fall into one of four main types—ZA, ZN, ZE (or ZI) and ZK types.

The worm-type hob cutter is one of the most popular cutting tools used in industry for worm gear manufacturing. Design criteria, classification and regrinding limitations for oversize hob cutters were investigated by Wildhaber [1]. He applied surface curvatures to obtain an approximate tooth contact bearing diagram for worm gears cut by oversize hob cutters. Winter and Wilkesmann [2] and Bosch [3] proposed different methods for obtaining more precise worm surfaces. Simon [4] put forward a method to calculate the optimal values for rotational and tilt angles of grinding wheel axis in the manufacture of high precision hobs. Janninck [5] suggested a method for predicting the initial contact pattern and showed the results by using a surface separation topological diagram over the entire worm gear surface. Colbourne [6] proposed a method for designing oversize hob cutters to cut worm gears. The contact surface separation topology concept was also adopted to show the results of his design. Bär [7] investigated the basic geometry of worm surfaces, and also studied grinding wheel surfaces and undercut problems. Kin [8] investigated limitations on worms to avoid undercutting, and also studied the envelope existence of contact lines. Litvin and Kin [9] also proposed a generalized tooth contact analysis (TCA) algorithm to determine the position of transfer points where ideal contact lines turn into real contact points. The influences of rotation axes misalignment and centre-distance offsets on conjugate worm gear sets were also investigated in their study. Simon [10] extended his research to the design of hobs for worm gear manufacturing with circular profiles. Pencil-type milling cutters and disk-type grinding wheels with relief grinding were also studied in his research. Colbourne [11] investigated undercutting, interference and non-conjugate contact in ZK-type worm gear sets. In his study, worm gear surfaces were obtained by considering the worm's surface as a series of rack cutters in an axial

†Department of Mechanical Engineering, National Chiao Tung University, Hsinchu, 30050, Taiwan.
*Author to whom correspondence should be addressed.

section. Kin [12] studied the surface deviations of the manufactured worm gear tooth surfaces when hob cutters had cutting-edge deviations. Tolerances for worm gear tooth profiles can also be obtained by applying Kin's method.

Theoretically, the worm gear of a conjugate worm gear set is cut with a worm-type hob cutter, and the gear set is in line contact. However, oversize worm-type hob cutters are widely used in industry for worm gear manufacturing, and bearing contacts of the worm gear sets thus produced are point contacts rather than line contacts. The term "oversize hob cutters" indicates the pitch diameter of the hob cutter is larger than that of the mating worm. Due to tooth-surface elasticity, the gear tooth contact area spreads under a load, usually covering an elliptical area in the neighborhood of the contact point. The tooth contacts thus form a set of contact ellipses, moving over tooth surfaces as the gears mesh. Consequently, the contact position of the worm gear set is sensitive to misalignment of the gear-rotation axes.

Influences of grinder profiles and tool settings on hob and worm production have been well studied in previous researches. However, the influences of hob cutter regrinding and tool-setting on worm gear manufacture have never been investigated. In this paper, a mathematical model for a ZE-type worm gear set is proposed. The worm gear of the proposed gear set was produced using an oversize worm-type hob cutter. Bearing contacts and kinematic errors in the worm gear set were determined by applying a proposed mathematical model of the worm gear set, and by using a tooth contact analysis (TCA) computer program. Surface separation topology techniques and an optimization theorem were also adopted to determine the optimum shape and locus of bearing contacts. Bearing contacts can be located in a desirable region of the worm gear surface by choosing a suitable setting distance and angle of the hob cutter. The influences of oversize hob cutter regrinding and setting adjustments on bearing contacts and kinematic errors in the ZE-type worm gear set were also studied. Minimization of kinematic errors and optimization of bearing contacts achieved by choosing an optimum hob cutter setting and by modifying the normal tooth angle of the mating worm were also investigated. A numerical example is given to demonstrate the determination of bearing contacts and kinematic errors in the ZE-type worm gear set. The proposed analysis procedures and the developed computer programs are most helpful in designing, analysing and manufacturing worm gear sets and oversize hob cutters.

2. GENERAL CONCEPT AND A MATHEMATICAL MODEL OF A ZE-TYPE WORM GEAR SET

Our main purpose was to investigate the effects of oversize hob cutter regrinding and tool setting on ZE-type worm gear manufacturing, especially the effects on bearing contacts and kinematic errors in the produced worm gear sets. Therefore for simplicity we omit the mathematical model derivation process for ZE-type worm gear sets. Only the surface equations for ZE-type worms and worm gears are presented.

A ZE-type worm can be cut on a lathe using a straight-edged cutter when a cylindrical gear-blank is rotating and the cutter is translating along the gear-blank rotation axis. Theoretically the ZE-type worm surface can be considered as the screw motion of a straight line tangent to the helix of the screw surface on its base cylinder. A mathematical model of the ZE-type worm was proposed by Litvin [13]. When we consider the two sides of the ZE-type worm surfaces, the position vector $\mathbf{R}^{(1)}$ and unit normal vector $\mathbf{n}^{(1)}$ can be modified and expressed as follows:

$$\mathbf{R}^{(1)} = \begin{bmatrix} r_b\cos\varphi_1 & \mp & l_1\cos\beta_b\sin\varphi_1 \\ r_b\sin\varphi_1 & \pm & l_1\cos\beta_b\cos\varphi_1 \\ P\varphi_1 & \pm & l_1\sin\beta_b \mp e \end{bmatrix} \tag{1}$$

and

$$\mathbf{n}^{(1)} = \begin{bmatrix} \sin\varphi_1 \sin\beta_b \\ -\cos\varphi_1 \sin\beta_b \\ \cos\beta_b \end{bmatrix} \tag{2}$$

where

$$e = \frac{t_x}{2} + \sqrt{r_1^2 - r_b^2}\tan\beta_b - P\sin^{-1}\left(\frac{l_1\cos\beta_b}{r_1}\right) \tag{3}$$

Parameter e is the compensation parameter that ensures the axial tooth width of the worm surface is equal to the desired width t_x. The plus and minus signs shown in Equation (1) are associated with the right-hand and left-hand sides of the respective worm surfaces. Parameters l_1 and φ_1 are two worm surface parameters, where l_1 represents the surface point along the straight-edge of the cutter and φ_1 is the rotation angle of the screw motion during cutting. β_b is the lead angle of the worm measured on the base cylinder and P is the lead, per radian revolution, of the worm. Parameter t_x is the axial tooth width of the worm measured on its pitch cylinder and r_b is the base radius of the ZE-type worm cylinder. In practice, worm gears are produced using oversize hob cutters. Based on the theory of gearing, the equation of meshing between a ZE-type oversize hob cutter and the manufactured worm gear can be derived and represented as follows:

$$l_2 = [\pm((r_b\cot\beta_b + S_h\cot\gamma)\cot(\phi + \varphi_2) - P\varphi_2) + e]\sin\beta_b \pm \left(\frac{1 - m_{21}\cos\gamma}{m_{21}\sin\gamma}\right. \tag{4}$$
$$\left. P - S_h\right)\frac{\cos\beta_b}{\sin(\phi + \varphi_2)}$$

where S_h is the hob cutter setting distance (i.e. the shortest centre distance between the rotation axes of the hob cutter and the produced worm gear), and γ is the setting angle of the hob cutter (i.e. the crossing angle formed by the rotation axes of the hob cutter and produced worm gear). Parameter ϕ is the rotation angle of the hob cutter during the worm gear cutting process and φ_2 is the corresponding worm gear rotation angle. The position vector $\mathbf{R}^{(2)}$ and unit normal vector $\mathbf{n}^{(2)}$ of the ZE-type worm gear are derived and expressed as follows:

$$\mathbf{R}^{(2)} = \begin{bmatrix} (r_b\cos\gamma\sin\phi_g \mp l_2\cos\phi_g\cos\beta_b\sin(\phi + \varphi_2) \\ \quad + (\pm l_2\sin\beta_b \mp e) + P\varphi_2)\sin\gamma\sin\phi_g + (\pm l_2\cos\gamma\cos\beta_b\sin\phi_g \\ \quad + r_b\cos\phi_g)\cos(\phi + \varphi_2) - S_h\cos\phi_g \\ (r_b\cos\gamma\sin\phi_g \pm l_2\cos\phi_g\cos\beta_b\sin(\phi + \varphi_2) \\ \quad + (\pm l_2\sin\beta_b \mp e) + P\varphi_2)\sin\gamma\sin\phi_g + (\pm l_2\cos\gamma\cos\beta_b\cos\phi_g \\ \quad - r_b\sin\phi_g)\cos(\phi + \varphi_2) + S_h\cos\phi_g \\ (-r_b\sin(\phi + \varphi_2) \mp l_2\cos(\phi + \varphi_2)\cos\beta_b\sin\gamma + (\pm l_2\sin\beta_b \mp e + P\varphi_2)\cos\gamma \end{bmatrix} \tag{5}$$

and

$$\mathbf{n}^{(2)} = \begin{bmatrix} (-\cos\gamma\cos(\phi + \varphi_2) + \sin\gamma\cot\beta_b)\sin\phi_g + \sin(\phi + \varphi_2)\cos\phi_g \\ (-\cos\gamma\cos(\phi + \varphi_2) + \sin\gamma\cot\beta_b)\cos\phi_g - \sin(\phi + \varphi_2)\sin\phi_g \\ \cos(\phi + \varphi_2)\sin\gamma + \cos\gamma\cot\beta_b \end{bmatrix} \tag{6}$$

where ϕ and ϕ_g are the motion parameters of the hob cutter and worm gear, respectively. These two parameters can be related by

$$\phi_g = \frac{|\omega_2|}{|\omega_1|}\phi = m_{21}\phi = \frac{N_1}{N_2}\phi \tag{7}$$

where m_{21} is the rotation ratio of the worm gear set, and N_1 and N_2 are the tooth numbers of the worm and worm gear, respectively.

3. TOOTH CONTACT ANALYSIS OF ZE-TYPE WORM GEAR SETS

Tooth contact analysis (TCA) of the worm and worm gear can be simulated by considering the meshing mechanism of the worm gear set, as shown in Fig. 1. Coordinate systems $S_1(X_1, Y_1, Z_1)$ and $S_2(X_2, Y_2, Z_2)$ are rigidly attached to the worm and worm gear, respectively. Coordinate systems $S_w(X_w, Y_w, Z_w)$ and $S_g(X_g, Y_g, Z_g)$ are reference coordinate systems for the worm and worm gear, respectively. When the worm rotates by angle ϕ_1, the worm gear will rotate through angle ϕ_2. Parameter S_E is the shortest centre distance between the worm axis Z_1 and the worm gear axis Z_2, and γ_w is the crossing angle formed by these two axes. To perform TCA on a worm gear set, position vectors and normal vectors of the mating worm and worm gear surfaces must be expressed in the same reference coordinate system, as for example coordinate system $S_w(X_w, Y_w, Z_w)$, as shown in Fig. 1. According to Fig. 1, the position vector and unit normal vector of the worm surface, represented in the coordinate system S_w, can be obtained by applying the following homogeneous coordinate transformation matrix equations:

$$\mathbf{R}_w^{(1)} = [M_{w1}]\mathbf{R}^{(1)}$$

and

$$\mathbf{n}_w^{(1)} = [L_{w1}]\mathbf{n}^{(1)} \tag{8}$$

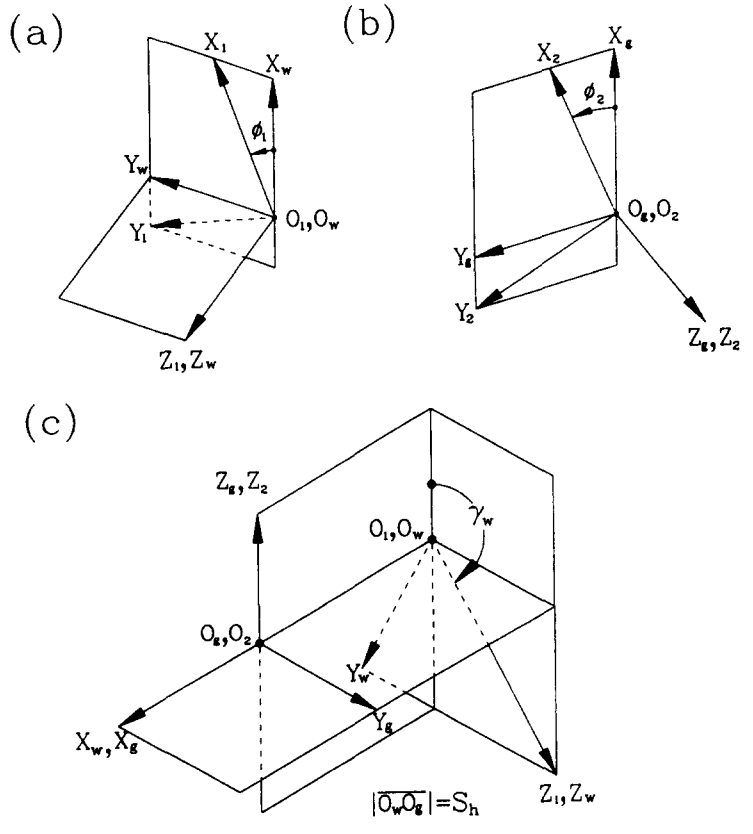

Fig. 1. Relationship between the worm and worm gear.

where

$$[M_{w1}] = \begin{bmatrix} \cos\phi_1 & -\sin\phi_1 & 0 & 0 \\ \sin\phi_1 & \cos\phi_1 & 0 & 0 \\ 0 & 0 & 1 & 0 \\ 0 & 0 & 0 & 1 \end{bmatrix}$$

and ϕ_1 is the rotation angle of the worm. $[M_{w1}]$ is the position transformation matrix that transforms from coordinate system S_1 to coordinate system S_w, and $[L_{w1}]$ is the vector transformation matrix obtained by deleting the last column and last row of matrix $[M_{w1}]$. Substituting Equations (1) and (2) into Equation (8), the worm surface and its unit normal represented in coordinate system S_w can be simplified as follows:

$$\begin{aligned} x_w^{(1)} &= r_b\cos(\phi_1 + \varphi_1) \mp l_1\sin(\phi_1 + \varphi_1)\cos(\beta_b) \\ y_w^{(1)} &= r_b\sin(\phi_1 + \varphi_1) \pm l_1\cos(\phi_1 + \varphi_1)\cos(\beta_b) \\ z_w^{(1)} &= P\varphi_1 \pm l_1\sin(\beta_b) \mp e \end{aligned} \tag{9}$$

and

$$\begin{aligned} n_{wx}^{(1)} &= \sin(\phi_1 + \varphi_1)\sin(\beta_b) \\ n_{wy}^{(1)} &= -\cos(\phi_1 + \varphi_1)\sin(\beta_b) \\ n_{wz}^{(1)} &= \cos(\beta_b) \end{aligned} \tag{10}$$

Similarly, the position and unit normal vectors of the worm gear surface, represented in the coordinate system by S_w, can be obtained by applying the following transformation matrix equations:

$$\mathbf{R}_w^{(2)} = [M_{w2}]\mathbf{R}^{(2)} \tag{11}$$

and

$$\mathbf{n}_w^{(2)} = [L_{w2}]\mathbf{n}^{(2)}$$

where

$$[M_{w2}] = \begin{bmatrix} \cos\phi_2 & -\sin\phi_2 & 0 & S_E \\ \cos\gamma_w\sin\phi_2 & \cos\gamma_w\cos\phi_2 & -\sin\gamma_w & 0 \\ \sin\gamma_w\sin\phi_2 & \sin\gamma_w\cos\phi_2 & \cos\gamma_w & 0 \\ 0 & 0 & 0 & 1 \end{bmatrix}$$

and ϕ_2 is the rotation angle of the worm gear. $[M_{w2}]$ is the position transformation matrix that transforms from coordinate system S_2 to coordinate system S_w, and $[L_{w2}]$ is the vector transformation matrix obtained by deleting the last column and last row of matrix $[M_{w2}]$. Substituting Equations (5) and (6) into Equation (11), the worm gear surface and its unit normal vectors represented in the coordinate system S_w can be simplified as follows:

$$
\begin{aligned}
x_w^{(2)} &= (\mp l_2\cos(\phi_2 - \phi_g)\cos\beta_b - r_b\sin(\phi_2 - \phi_g)\cos\gamma)\sin(\phi + \varphi_2) \\
&\quad + (r_b\cos(\phi_2 - \phi_g) \mp l_2\sin(\phi_2 - \phi_g)\cos\gamma\cos\beta_b)\cos(\phi + \varphi_2) \\
&\quad + S_E - S\cos(\phi_2 - \phi_g) - (\pm l_2\sin\beta_b \mp e + P\varphi_2)\sin(\phi_2 - \phi_g)\sin\gamma \\
y_w^{(2)} &= \{(r_b\sin(\phi_2 - \phi_g) \pm l_2\cos(\phi_2 - \phi_g)\cos\beta_b\cos\gamma)\cos(\phi + \varphi_2) \\
&\quad - (r_b\sin(\phi_2 - \phi_g)\cos\gamma \pm l_2\cos(\phi_2 - \phi_g)\cos\beta_b)\sin(\phi + \varphi_2) \\
&\quad + (P\varphi_2 \pm l_2\sin\beta_b \mp e)\cos(\phi_2 - \phi_g)\sin\gamma - S\sin(\phi_2 - \phi_g)\}\cos\gamma_w \\
&\quad + \{r_b\gamma\sin(\phi + \varphi_2) \pm l_2\cos(\phi + \varphi_2)\cos\beta_b\sin\gamma - (P\varphi \pm l_2\sin\beta_b \mp e)\}\sin\gamma_w \\
z_w^{(2)} &= \{(r_b\sin(\phi_2 - \phi_g) \pm l_2\cos(\phi_2 - \phi_g)\cos\beta_b\cos\gamma)\cos(\phi + \varphi_2) \\
&\quad - (r_b\sin(\phi_2 - \phi_g)\cos\gamma \pm l_2\cos(\phi_2 - \phi_g)\cos\beta_b)\sin(\phi + \varphi_2) \\
&\quad + (P\varphi_2 \pm l_2\sin\beta_b \mp e)\cos(\phi_2 - \phi_g)\sin\gamma - S\sin(\phi_2 - \phi_g)\}\sin\gamma_w \\
&\quad + \{r_b\sin\gamma\sin(\phi + \varphi_2) \pm l_2\cos(\phi + \varphi_2)\cos\beta_b\sin\gamma - (P\varphi_2 \pm l_2\sin\beta_b \mp e)\}\cos\gamma_w
\end{aligned}
\tag{12}
$$

and

$$
\begin{aligned}
n_{xw}^{(2)} &= (\cos(\phi_2 - \phi_g)\sin(\phi + \varphi_2) \\
&\quad + \sin(\phi_2 - \phi_g)\cos(\phi + \varphi_2)\cos\gamma)\sin\beta_b \\
&\quad - \sin(\phi_2 - \phi_g)\sin\gamma\cos\beta_b \\
n_{yw}^{(2)} &= [(\sin(\phi_2 - \phi_g)\sin(\phi + \varphi_2) - \cos(\phi_2 - \phi_g)\cos(\phi + \varphi_2)\cos\gamma)\sin\beta_b \\
&\quad + \cos(\phi_2 - \phi_g)\sin\gamma\cos\beta_b]\cos\gamma_w \\
&\quad - (\cos(\phi + \varphi_2)\sin\gamma\sin\beta_b + \cos\gamma\cos\beta_b)\sin\gamma_w \\
n_{zw}^{(2)} &= [(\sin(\phi_2 - \phi_g)\sin(\phi + \varphi_2) \\
&\quad - \cos(\phi_2 - \phi_g)\cos(\phi + \varphi_2)\cos\gamma)\sin\beta_b \\
&\quad + \cos(\phi_2 - \phi_g)\sin\gamma\cos\beta_b]\sin\gamma_w \\
&\quad - (\cos(\phi + \varphi_2)\sin\gamma\sin\beta_b + \cos\gamma\cos\beta_b)\cos\gamma_w
\end{aligned}
\tag{13}
$$

In the meshing process, worm and worm gear tooth surfaces are continuously tangent at every contact point. Therefore the following criteria must be observed at every contact point: (1) position vectors of the worm surface $\mathbf{R}_w^{(1)}$ and the worm gear surface $\mathbf{R}^{(2)}$ must be equal; (2) unit normal vectors of the worm surface $\mathbf{n}_w^{(1)}$ and the worm gear surface $\mathbf{n}_w^{(2)}$ must be the same. Based on Equations (8)–(13) and the above-mentioned meshing criteria, a system of five independent equations can be obtained:

$$x_w^{(1)} - x_w^{(2)} = 0 \tag{14}$$

$$y_w^{(1)} - y_w^{(2)} = 0 \tag{15}$$

$$z_w^{(1)} - z_w^{(2)} = 0 \tag{16}$$

$$n_{yw}^{(1)}n_{zw}^{(2)} - n_{zw}^{(1)}n_{yw}^{(2)} = 0 \tag{17}$$

$$n_{xw}^{(1)}n_{zw}^{(2)} - n_{zw}^{(1)}n_{xw}^{(2)} = 0 \tag{18}$$

Since $|\mathbf{n}_{wi}{}^{(1)}| = |\mathbf{n}_{wi}{}^{(2)}| = 1$, the meshing criterion of a ZE-type worm gear set consists of a system of five independent equations only. Equations (14)–(18) contain six unknowns: l_1, φ_1, φ_2, ϕ, ϕ_1 and ϕ_2. In solving a system of five equations with six unknowns, one of the unknowns must be chosen as a given parameter (i.e. input value). After solving the system of equations, contact point coordinates can be determined. Kinematic error in the worm gear set $\Delta\phi_2$is calculated using the following equation:

$$\Delta\phi_2 = (\phi_2 - \phi_{20}) - \frac{N_1}{N_2}(\phi_1 - \phi_{10}), \tag{19}$$

where ϕ_{10} and ϕ_{20} are the rotation angles of the worm and worm gear, respectively, at some reference contact points. N_1 and N_2 are the tooth numbers of the worm and worm gear, respectively.

4. SURFACE SEPARATION TOPOLOGY

In the mating process, worm and worm gear surfaces are tangent to each other at every instantaneous contact point. Therefore common tangent plane to the mating surfaces can be found at any contact point. In order to measure the separation value of the two surfaces along the normal direction of the tangent plane, the surface coordinates of the worm and worm gear must be transformed onto the common tangent plane. The relationship between the common tangent plane and the worm reference coordinate system $S_w(X_w, Y_w, Z_w)$ is shown in Fig. 2. The coordinate system $S_\tau(X_\tau, Y_\tau, Z_\tau)$ is associated with the common tangent plane, and the Z_τ-axis is coincident with the normal direction of the tangent plane. $\mathbf{R}_w$ is the position vector of the common contact point represented in the S_w coordinate system. The position and unit normal vectors of the worm and worm gear surfaces represented in the coordinate system S_τ can be obtained by applying the following coordinate transformation matrix equation:

$$\mathbf{R}_\tau^{(i)} = [M_{\tau w}]\mathbf{R}_w^{(i)} \tag{20}$$

and

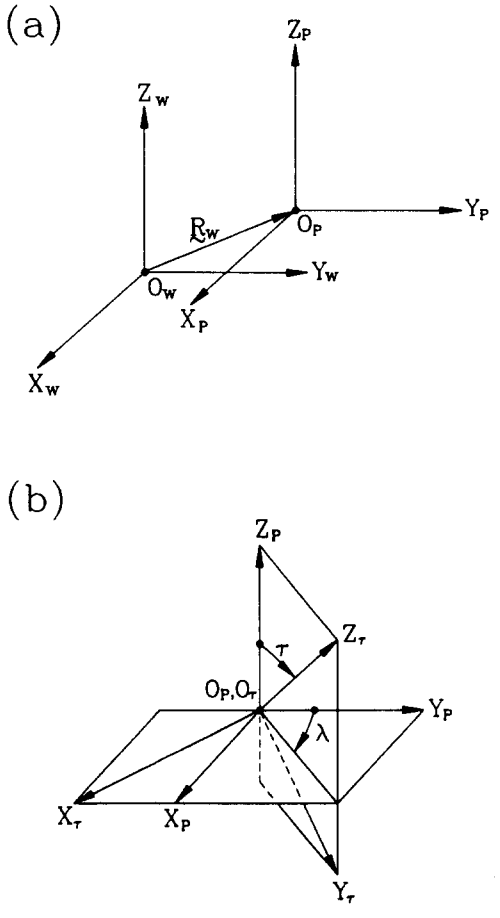

Fig. 2. Coordinate systems of the contact point and common tangent plane.

$$\mathbf{n}_\tau^{(i)} = [L_{\tau w}]\mathbf{n}_w^{(i)}$$

where

$$[M_{\tau w}] = \begin{bmatrix} \cos\lambda & -\sin\lambda & 0 & y_p\sin\lambda - x_p\cos\lambda \\ \cos\tau\sin\lambda & \cos\tau\cos\lambda & -\sin\tau & z_p\sin\tau - x_p\cos\tau\sin\lambda - y_p\cos\tau\cos\lambda \\ \sin\tau\sin\lambda & \sin\tau\cos\lambda & \cos\tau & -z_p\cos\tau - x_p\sin\tau\sin\lambda - y_p\sin\tau\cos\lambda \\ 0 & 0 & 0 & \end{bmatrix}$$

and matrix $[[L_{\tau w}]]$ can be obtained by deleting the last column and last row of the matrix $[M_{tw}]$. Symbols x_p, y_p and z_p are coordinates of the contact point represented in the coordinate system S_w. In Equation (20), the position and normal vectors of the worm and worm gear surfaces can be expressed by replacing the superscript "i" with "1" and "2", respectively. Transformation angles λ and τ of the common tangent plane are expressed by the following equations:

$$\lambda = \tan^{(-1)}\left(\frac{n_{xw}^{(1)}}{n_{yw}^{(1)}}\right) \tag{21}$$

and

$$\tau = \cos^{(-1)}n_{zw}^{(1)} \tag{22}$$

where $n_{xw}^{(1)}$, $n_{yw}^{(1)}$ and $n_{zw}^{(1)}$ are projection components of the worm surface unit normal represented along the three axes of the S_w coordinate system. The separation value ε of the two mating surfaces can be measured along the Z_τ-axis (i.e. the normal direction of the tangent plane), and can be calculated by applying the following equations:

$$\varepsilon = z_\tau^{(1)} - z_\tau^{(2)} \tag{23}$$

$$x_\tau^{(1)} - x_\tau^{(2)} = 0 \tag{24}$$

and

$$y_\tau^{(1)} - y_\tau^{(2)} = 0 \tag{25}$$

Based on a prescribed separation value, the contour of the contact ellipses can be determined by applying the contouring algorithm.

5. NUMERICAL EXAMPLE

A worm gear set with a transmission ratio of 1:33 was chosen for the demonstrative example. The major design parameters of the worm gear set are given as follows: (1) tooth numbers of the worm and oversize hob cutter N_1 = one tooth; (2) modules of the worm and oversize hob cutter m = 8.5 mm tooth^{-1}; (3) crossing angle of the worm gear set $\gamma_1 = 90°$; (4) pitch diameter of the of the worm d_1 = 79.5 mm; (5) half apex-angle of the straight-edged cutting blade $\alpha = 20°$; and (6) pitch diameter of the oversize hob cutter d_1 = 85.00 mm. The profile of the oversize hob cutter is based on the concept that the tooth widths of the worm and hob cutter are equal in their normal sections on the pitch cylinder. In order to satisfy this criterion, the theoretical setting angle γ of the oversize hob cutter in the cutting process must be smaller than that of the worm in the meshing process (i.e. angle γ_1), as shown in Fig. 1, and it can be calculated by applying the following formula:

$$\gamma = \gamma_1 - \beta_1 + \beta_0 = 89°35'59' \tag{26}$$

where β_1 and β_0 are the lead angles of the worm and oversize hob cutter, respectively. Based on the developed mathematical model of the worm gear set, the contact surface topology method and the TCA computer simulation programs, the bearing contact of worm gear sets can be obtained. In practice, worm gears are cut using oversize worm-type hob cutters, and the profiles of the hob cutters are the same as those of the worms. Figure 3(a)–(c) shows the bearing contacts on the worm gear surfaces when pitch diameters of the oversize hob cutter were 85.00 mm (6.92% oversize), 79.63 mm (0.16% oversize) and 79.50 mm (not oversized), respectively. It is worth mentioning that line contact occurred when the pitch diameters of the hob cutters were reground to 79.50 mm, which is equal to the pitch diameter of the worm. Here the worm gear set became a conjugate kinematic pair rather than a pseudo-conjugate gear pair, and the kinematic error was zero. In this example the separation value of bearing contours was set at 0.00635 mm, which is the size of coating particles usually used in rolling-test experiments. Figure 4 shows the kinematic errors in worm gear sets, made with hob cutters 85.00 and 79.63 mm oversize in pitch diameter, are 0.289 and 0.021 sec arc, respectively. Influences of assembly errors on a ZE-type worm gear set were investigated when the worm gear was cut using an oversize hob cutter with a pitch diameter of 85.00 mm and a mated worm having a pitch diameter of

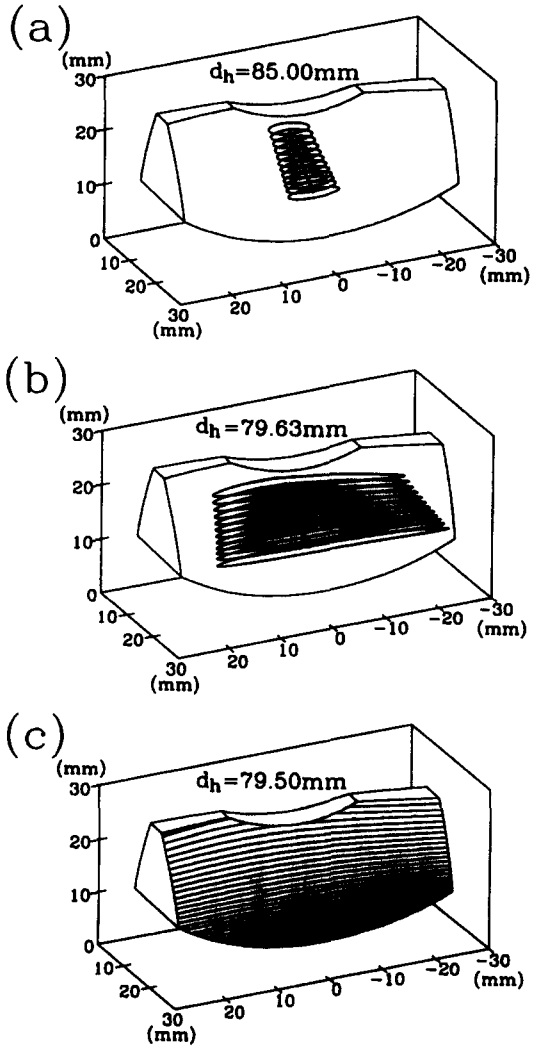

Fig. 3. Bearing contacts and contact paths of a ZE-type worm gear set using different oversize hob cutter pitch diameters.

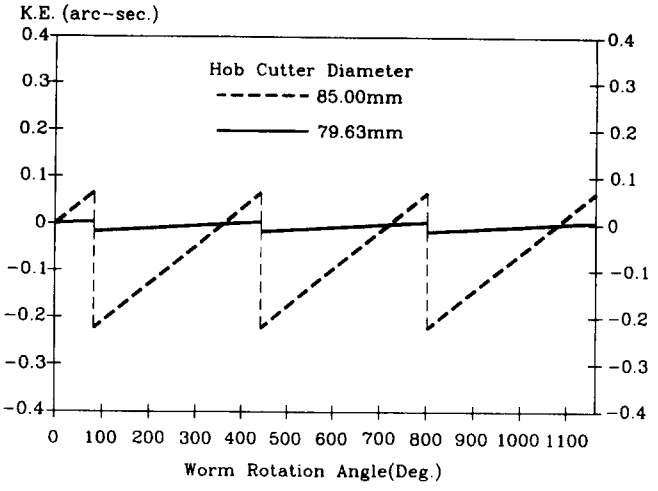

Fig. 4. Kinematic errors in a ZE-type worm gear set using different oversize hob cutter pitch diameters.

79.50 mm. Figure 5(a) shows the bearing contacts of a worm gear set when the hob cutter had a 2.0 mm centre-distance variation (1.094% centre-distance error) during the worm gear cutting process, and Fig. 5(b) shows that its corresponding kinematic error is 0.289 sec arc. Figure 6(a) shows the bearing contacts of a worm gear set when the hob cutter had $-0.2°$ crossing angle misalignment during the worm gear cutting process, and Fig. 6(b) shows that its corresponding kinematic error is also 0.289 sec arc. Figure 7(a) shows the relationship between the kinematic error and the normal tooth angle of a mating worm, and Fig. 7(b) shows the bearing contacts of a worm gear set when the normal tooth angle of the mating worm was modified to 20.001158817°. It is worth mentioning that under this normal tooth-angle modification the kinematic error was zero. However, the path and locations of bearing contacts were still not satisfactory. If the hob cutter setting adjustment were increased by 2.0 mm in the centre distance and decreased by 0.34° in the crossing angle, bearing contacts of the worm gear set could be as shown in Fig. 8.

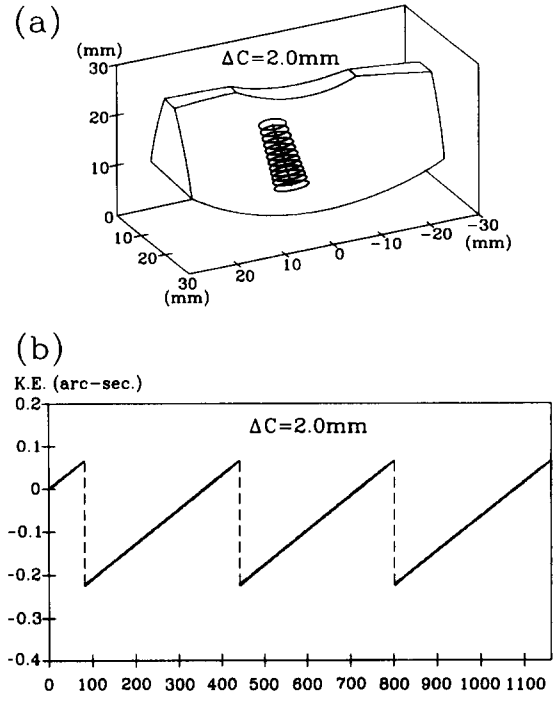

Fig. 5. Bearing contacts and kinematic errors in a ZE-type worm gear set with centre-distance variation during the worm gear cutting process.

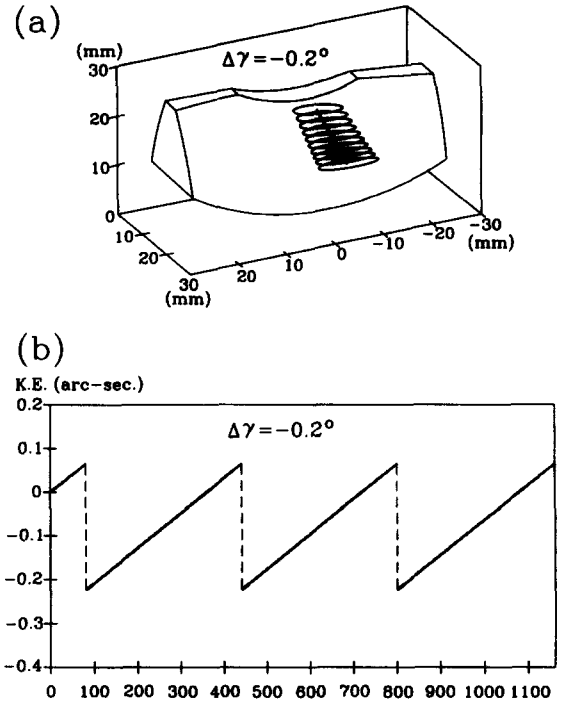

Fig. 6. Bearing contacts and kinematic errors in a ZE-type worm gear set with axes misalignments during the worm gear cutting process.

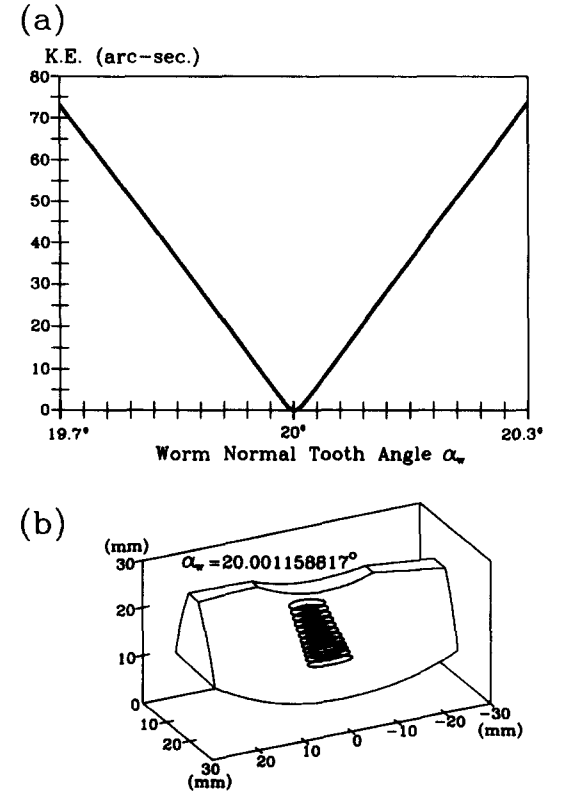

Fig. 7. (a) Relationship between worm normal tooth angle and kinematic errors; (b) bearing contact with a modified worm normal tooth angle.

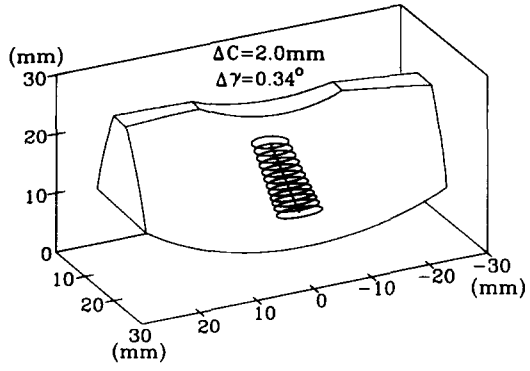

Fig. 8. Bearing contacts with the modified tool-settings.

6. DISCUSSION

When an oversize hob cutter is reground to a smaller pitch diameter, the contact ellipse of the produced worm gear set will be spread over a longer contact shape, as shown in Fig. 3. This phenomenon complies with the fact that line contact occurs and kinematic error is zero for a conjugate mating worm gear pair when the pitch diameter of the oversize hob cutter is reground and decreased to equal that of the worm. As shown in Fig. 4, the level of kinematic error of the produced worm gear set will be lower if a smaller pitch diameter of the oversize hob cutter is used to cut the worm gear. As demonstrated in Fig. 3(a), if the pitch diameter of an oversize hob cutter is larger than 85.00 mm, the area of bearing contact will be too small to carry a heavy load. However, if the pitch diameter of an oversize hob cutter is smaller than 79.76 mm, edge contact will occur and edge failure may happen. For these reasons, the working life (i.e. regrinding) of the hob cutter should be limited to from 6.92 to 0.16% of an oversized pitch-diameter.

If the hob cutter has a 1.094% centre-distance variation, bearing contact will be located near the central area of the worm gear surface, as shown Fig. 5(a). Comparing Fig. (4) with Fig. 5(b), the hob cutter centre-distance variation has no effect on kinematic errors. If the hob cutter has $-0.2°$ crossing angle misalignment, bearing contact will be shifted to the right-hand side of the worm gear surfaces. Comparing Fig. (4) with Fig. 6(b), the hob cutter crossing angle misalignment also has no effect on kinematic errors. As shown in Fig. 7(a), kinematic errors in the worm gear set can be minimized by choosing a mating worm with a suitable normal tooth angle. Changing the normal tooth angle of the mating worm has no influence on the location of bearing contact, as illustrated in Fig. 7(b).

Due to the characteristics of hob cutter setting adjustments and the worm tooth profile modifications mentioned above, the procedures for bearing contact optimization can be divided into two steps: (1) adjust the hob cutter setting parameters to obtain an acceptable contact pattern and a suitable area location; (2) modify the normal tooth angle of the mating worm to minimize kinematic error. Based on the optimization theorem, the bearing contacts shown in Fig. 3(a) can be located in the central area of the worm gear surface by adjusting the hob cutter setting by a 2.0 mm centre-distance increment and a $-0.34°$ crossing angle setting. The kinematic error of the gear set can then be reduced to zero by modifying the normal tooth angle of the mating worm to $\alpha_w = 20.001158817°$.

7. CONCLUSION

Based on the proposed mathematical model and TCA techniques, bearing contact and kinematic error due to the regrinding of oversize hob cutters have been investigated. The profile and dimensions of contact ellipses are most helpful in stress and lubrication analyses of the worm gear set, and in the working-life estimations of oversize hob cutters. The effects of hob cutter setting modification can also be obtained by applying the developed TCA computer programs. Kinematic errors in worm gear sets can also be minimized by modifying the normal tooth angle of mating worms. An optimum bearing contact and

worm gear set contact path can be successfully implemented by adjusting the hob cutter tool-setting and modifying the worm normal tooth angle.

Acknowledgements—The authors are grateful to the National Science Council of the Republic of China for their grant. Part of this work was performed under contract no. NSC-84-2212-E009-016.

REFERENCES

[1] E. Wildhaber, *A New Look at Worm Gear Hobbing*, 129.10. American Gear Manufactures Association, Virginia (1954).
[2] H. Winter and H. Wilkesmann, Calculation of cylindrical worm gear drives of different tooth profiles, *J. Mech. Des.* **103**, 73 (1981).
[3] M. Bosch, *Economical Production of High Precision Gear Worms and Other Thread Shaped Profiles by Means of CNC-Controlled Worm and Thread Grinding Machines*, p. 3. Klingelnberg, Hükeswagen, Germany (1988).
[4] V. Simon, Computer-aided manufacturing of high precision hobs, *Int. J. Mach. Tools Manufact.* **28**, 443 (1988).
[5] W. L. Janninck, Contact surface topology of worm gear teeth. *Gear Technol.* March/April, 31 (1988).
[6] J.R. Colbourne, *The Use of Oversize Hobs to Cut Worm Gears*. American Gear Manufactures Association, Virginia (1989).
[7] G. Bar, CAD of worms and their machining tools, *Comput. Graphics* **14**, 405 (1990).
[8] V. Kin, Limitations of worm and worm gear surfaces in order to avoid undercutting. *Gear Technol.* November/December, 30 (1990).
[9] F. L. Litvin and V. Kin, Computerized simulation of meshing and bearing contact for single-enveloping worm-gear drives, *ASME J. Mech. Des.* **114**, 313 (1992).
[10] V. Simon, Hob for worm gear manufacturing with circular profile, *Int. J. Mach. Tools Manufact.* **33**, 615 (1993).
[11] J. R. Colbourne, *Undercutting in Worm and Worm-gears*, 93FTMI. American Gear Manufactures Association, Virginia (1993).
[12] V. Kin, *Topological Tolerancing of Worm-Gear Tooth Surfaces*, 93FTM2. American Gear Manufactures Association, Virginia (1993).
[13] F. L. Litvin, *Gear Geometry and Applied Theory*. Prentice Hall, Englewood Cliffs, NJ (1994).